Running Head Title: Drop tests for hypergolic EMIM SCN Reactions

THE HYPERGOLIC REACTION BETWEEN GREEN IONIC LIQUIDS AND HYDROGEN PEROXIDE IN A LAB-SCALE DROP TEST CHAMBER

Robert G. Stützer,[1,*] Jakob Balkenhohl,[1] Felix Lauck,[1] Michael Oschwald,[1] & Stefan Schlechtriem[1]

[1]DLR German Aerospace Center, Lampoldshausen, Baden-Württemberg, 74239, Germany

*Address all correspondence to: Robert G. Stützer, DLR German Aerospace Center, Lampoldshausen, Germany, 74239, E-mail: robert.stuetzer@dlr.de

Original Manuscript Submitted: 3/01/2021; Final Draft Received:

The hypergolic reaction between the recently developed green propellant combination consisting of an ionic liquid and highly concentrated hydrogen peroxide was investigated for several ratios of oxidizer and fuel, drop sizes and heights of fall. The influence of the catalytic copper additive on the ignition delay time (IDT) was analysed. Flame emission/absorption spectroscopy revealed the chemical constituents. All spectra were dominated by sodium D-lines at λ= 589nm. Further lines of alkali metals such as lithium and potassium were found. The copper additive showed its characteristic lines accordingly to its amount in the fuel. Emission spectra of the ultraviolet regime showed the characteristic OH molecular lines around λ= 306nm with its temperature dependent intensity ratios (De Izarra 2000; Pellerin et al. 1996). The catalytic additive copper increases the flame temperature while it decreases the IDT from 31 ms for pure ionic liquid to 15 ms (5% mass fraction).*

KEY WORDS: *green propellants, green propulsion, flame emission spectroscopy, hypergolic combustion*

1. INTRODUCTION

Hypergolic propellants are widely applied in space propulsion systems. Due to their storability, reliability, and ability for spontaneous ignition, these fuels are preferred for long time missions. The conventional hypergolic combustion process was investigated numerically (Nonnenberg et al. 2004; Catoire et al. 2004) as well as experimentally under laboratory (Catoire et al. 2006) and test bench conditions (Stützer et al. 2020; Stützer et al. 2013). However, the conventional hypergolic derivatives of hydrazine and the associated oxidizers are very toxic and harmful to the environment (Matsumoto et al. 2016; Mellor 2004). Therefore, efforts have been made to find and establish a less noxious replacement. Ionic liquids (IL) and highly concentrated hydrogen peroxide (HTP) are such promising candidates (Lauck et al. 2020). Hence, research on the ignition behavior, the influence of catalysts, and the combustion process itself is essential to understand and optimize the application of this fuel-oxidizer combination in satellite thrusters or launcher engines (Lauck et al. 2019). In order to establish an appropriated method for reproducible data acquisition, an optically accessible drop test chamber for hypergolic ignition experiments was designed, manufactured and applied (Lauck et al. 2021 (a); Balkenhohl 2019). Recently novel hypergolic propellant combinations consisting of hydrogen peroxide and ionic liquids with a thiocyanate anion were found (Lauck et al. 2021 (b)).

2. EXPERIMENTAL

Drop tests were conducted in compliance with safety regulations. All experiments took place in a ventilated fume hood that also protects against explosion and harming due to moving of small parts (FIG. 1).

2.1 Drop Test Chamber Design

Several requirements on the chamber design had to be identified in order to obtain sufficient output under reproducible conditions. These standards are derived from the scientific objectives the setup has to fulfil and the theoretical background of its constituents. Therefore, the chamber has to

- be fully enclosed and the height and size of the droplets have to be adjustable.
- has to withstand pressure peaks during ignition as well as pressure values of 0.3 bar or lower.
- be optically accessible for absorption and emission measurements from the UV to the NIR regime of photon wavelengths.
- be accessible for cleaning and maintenance.
- be remotely operable.
- be suited for a variety of chemical components.
- ensure inside temperature and pressure measurements.
- be light and compact enough in order to be easily moveable.
- cool the fuel and oxidizer if necessary.

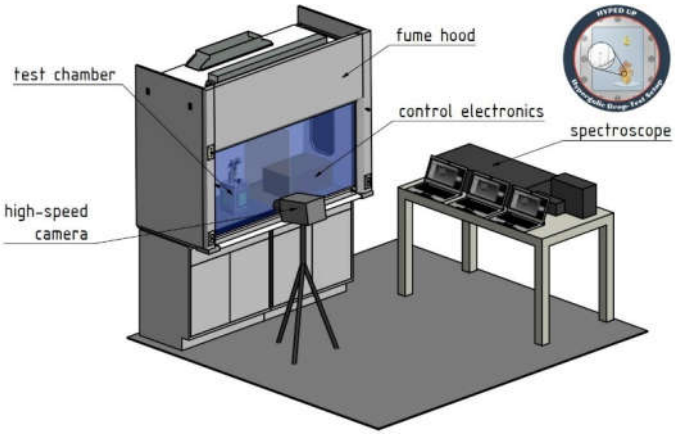

FIG. 1: Drop test setup with optical instruments.

The drop test chamber design is depicted in FIG. 2. It consists of a 216 mm long section of a 150 x 150 x 5 mm square aluminum profile with windows on three sides to allow optical access. One side has a panel that can be removed entirely to allow physical access. On the back side are connections for both water and vacuum pump. The open ends of the profile are closed with two 150 x 150 x 10 mm aluminum plates. Placed on top of the chamber is a syringe pump that is used to inject the propellants into the chamber. The top plate also has connections for a pressure transducer, a barometer, a thermocouple and a pipe to feed in the inert gas.

In order to allow for spectral analysis of the occurring combustion, the window glass must have a transmission of 90% or higher for wavelengths ranging from 300 nm to 800 nm. Furthermore, the glass thickness has to ensure a particular pressure resistance.

The syringe pump system is a central design aspect of the chamber. It determines the amount of fuel and oxidizer that react with each other. The system consists of a syringe, a cannula, and a watch glass dish. In order to create a reliable and constant drop size, medical cannulas are used.

The syringe creates a drop that falls onto the pre-dropped component that is stored in the watch glass.

An extinguishing/cleaning system operates automatically and remotely controllable using a metal bracket connected to a small motor in order to rotate the dish. A water nozzle connected to a pipe with an electromagnetic valve is placed below the dish. After combustion, the dish can be turned upside down and sprayed down by the nozzle to remove residue and extinguish flames.

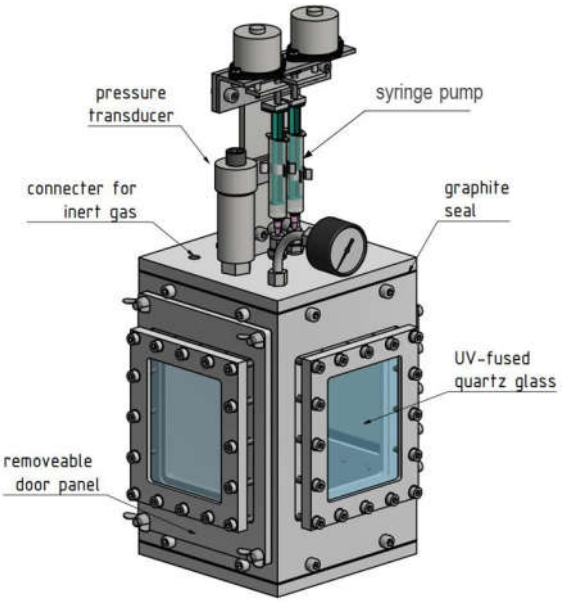

FIG. 2: Optically accessible drop test chamber for hypergolic ignition experiments.

2.2 High speed visualization

High speed video recording has been conducted in order to determine the drop impact and IDT using a Photron FastCam models SA5 and SA-X2. The former is a monochromatic camera which records with a frame rate of 7.000 Hz when using the full chip at a maximum resolution of 1024 x 1024 pixels. The model SA-X2 is a color camera provides a maximum frame rate of 12.500 Hz

when using the full sensor area of 1024 square pixels. Both camera systems are connected to a control computer and operated using the firm ware Photron FastCam Viewer (PFV) version 3.50. A 1.5 Watt LED attached to the camera is used to sufficiently illuminate the chamber interior. Furthermore, the lens aperture is slightly closed in order to increase the depth of field and thus to ensure proper focus of the drop impact place. A f = 100 mm lens is used, allowing the camera to be placed outside the fume hood on a stable tripod. In order to properly visualize the surface of the liquid at the bottom of the dish, the camera is placed at an angle pointing through the front window. At a frame rate of 3.600 fps and an exposure time of 3.600^{-1} s, the image is found to be sufficiently bright while providing a high enough temporal resolution for our purposes.

Using the PFV software, a trigger signal was created for the exact time when a change occurs in the viewing field of the camera. To do so, an area as well as a threshold was defined, that tells the software which percentage the average of the image bin entries in the above mentioned area should stray from the pre-determined background before the recording is triggered. This trigger signal is then passed to the spectrograph via BNC bus in order to trigger the camera and spectrograph system when the drop falls into the frame.

2.3 Flame emission spectroscopy

The spectroscopy subsystem consists of different components as shown in FIG. 3. We used the Princeton Instruments model SpectraPro2756 in combination with the PI-Max 2 intensified CCD (ICCD) camera and the ST133 controller. The SP2756 is a Czerny-Turner-design spectrograph with a focal length of 750 mm and an aspect ratio of f/9.7. It has an interchangeable triple grating turret with configuration properties listed in TABLE 1. The given linear dispersion and spectral coverage is for a focal plane of 26.8 mm. The SP2756 is configured with a side entrance slit for the incoming light and a front flange port where the split up light exits and the CCD camera is

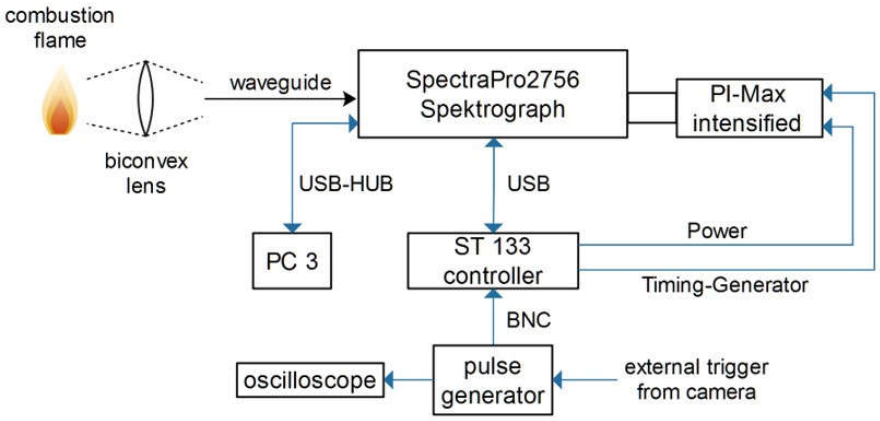

FIG. 3: Schematic of the spectroscopy system components.

attached. The slit width can be manually adjusted from 10 µm to 3 mm. The light signal coming from the flame emission is passed on out of the fume hood to the spectroscope via glass fiber waveguide.

The PI-Max 2 system consists of a CCD sensor and an image intensifier, housed inside the camera as well as the ST 133 controller. The CCD sensor is the CCD30-11 front-illuminated open electrode high-performance CCD sensor by e2v technologies. It has a size of 1024 x 256 pixels with a square pixel size of 26 µm, resulting in a total area of 26.6 x 6.7 mm. It is oriented in a way that the resulting spectral lines are parallel to the shorter side of the sensor. Its spectral range is from 200 to 1060 nm and it is specifically made for near UV spectroscopy applications. Its quantum efficiency is described elsewhere (CCD30-11 2013). The image intensifier is a HQf Gen III filmless intensifier that is fibre-optically coupled to the CCD array. It is a proximity-focused microchannel plate (MCP) image intensifier. Its width of 18 mm limits the total active surface area of the CCD intensifier combination to 18.0 x 6.7 mm.

TABLE 1: Spectrometer gratings and the resulting linear dispersion and coverage.

Grating [gr./mm]	**Blaze** [nm]	**Lin. dispersion** [nm/mm]	**sp. range** [mm]
150	500	8.8	235
600	500	2.16	57
1800	500	0.64	17

The camera head is cooled by a multi-stage peltier element and a cooling fan. The ST133 controller provides the high voltages required for the intensifier and controls the exposure timing, scan control and temperature of the ICCD.

3. RESULTS AND DISCUSSION

The presented drop tests were conducted with 96.1 wt.% hydrogen peroxide and the ionic liquid 1-ethyl-3-methylimidazolium thiocyanate (EMIM SCN). As additive copper (I) thiocyanate (Cu SCN) was used. A few millilitres of one of the two propellant components were stored on the glass dish inside the drop chamber. In order to induce the hypergolic ignition, a well-defined amount of the second component was then dropped onto the same dish which triggered the optical instruments for measurement (FIG. 4).

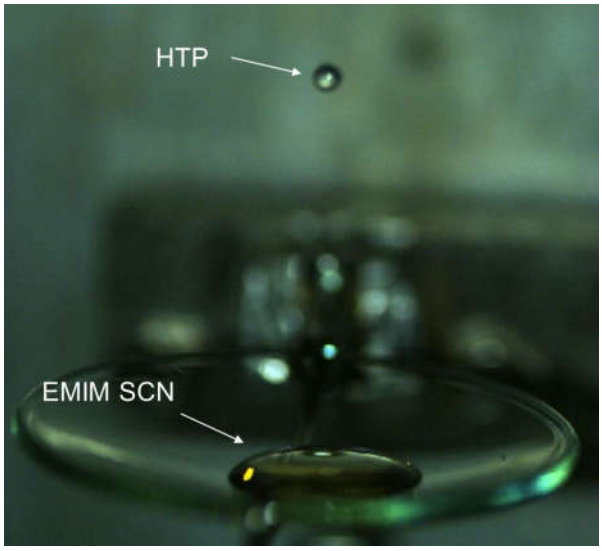

FIG. 4: Before ignition: A drop of high-test peroxide (HTP) falls onto the ionic liquid EMIM SCN.

3.1 Ignition process visualization

Using a high-speed camera system the ignition process and flame development were recorded and analyzed. Decisive moments and time regimes are depicted in FIG. 5. The moment of contact between fuel and oxidizer is defined as t_0 (Lauck et al. 2021 (a); Balkenhohl 2019). The touchdown impact depends on drop size and height of fall, i.e. mass and velocity.

Hence, instantly after the first contact between both constituents, the mixing phase begins. After several milliseconds, exothermal chemical reactions induce a rapid heating and the phase transition from liquid to the gaseous state. Once the ignition temperature is reached, a highly energetic explosion occurs with a characteristic flame emission.

The time between first contact of oxidizer and fuel and the explosive ignition is defined as the ignition delay time (IDT). However, in order to guarantee a smooth and safe combustion, it is the

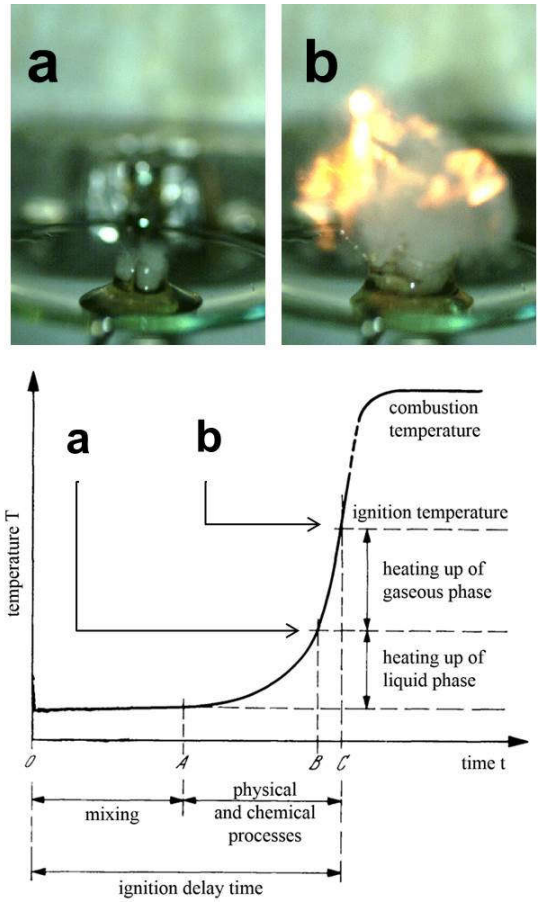

FIG. 5: Ignition process and flame development. Frame a shows the liquid-gas phase transition while both constituents are still heating up. Frame b depicts the moment of ignition at the temperature threshold. This time after touchdown at t_0 defines the ignition delay time (IDT) (Lauck et al. 2021 (a); Balkenhohl 2019).

goal to shorten the IDT as much as possible. Using the catalytic properties of a copper additive, the hence decreased ignition threshold was examined using optical methods.

All experiments were carried out under ambient pressure and temperature conditions.

3.2 Ignition delay time manipulation

Not only was the particular influence of the catalyst copper examined; the general impact of drop size and height, drop order and mixture ratio on the IDT was also investigated. TABLE 2 depicts results of IDT measurements for various parameters. Each result is an averaged value of at least 30 single measurements. Obviously, the ignition delay time IDT is reduced by half when a drop of the oxidizer HTP falls onto the liquid fuel, compared with *vice versa*. The impact velocity (drop height), on the other hand, does not essentially affect the IDT. A more detailed analysis can be found in (Balkenhohl et al. 2021 (a)).

However, the addition of the catalyst copper to the liquid fuel EMIM SCN has a significant effect on reducing the IDT (TABLE 2). While the entire lack of a catalyst results in an IDT of 31.3 ± 3.8 ms, reduces a weight percentage of 1% of Cu in the fuel the IDT to 16.2 ± 2.0 ms. Moreover, the addition of 5 wt.% Cu in the fuel decreases the IDT to 13.3 ± 1.1 ms, indicating a saturation effect in IDT reduction by adding this amount of the catalyst Cu.

TABLE 2: Ignition delay times (IDT) for varying amount of the copper additive, the drop order, ROF and drop height (impact velocity).

Additive content [wt.% Cu SCN]	**drop order**	**ROF**	**drop height** [mm]	**IDT** [ms]
-	O. on F.	0.12	61	31.3 ± 3.8
1	O. on F.	0.12	61	16.2 ± 2.0
5	O. on F.	0.12	61	13.3 ± 1.1
-	F. on O.	6.11	61	65.3 ± 7.0
-	O. on F.	0.12	141	31.0 ± 6.5

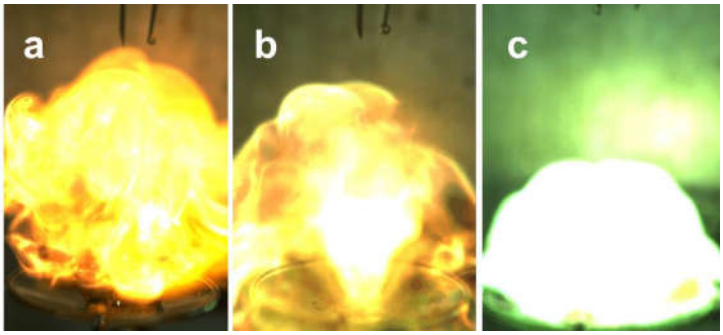

FIG. 6: Flame emission visualization of the reaction between HTP and the ionic liquid fuel EMIM SCN. The fuel consists no catalyst (a), 1 wt.% Cu (b), and 5 wt.% Cu (c).

The visual influence of Cu in the fuel is depicted in FIG. 6: An additional weight percentage of 5% in the fuel results in green flame emission. The plain flame emits mainly in the yellowish wavelength regime.

3.3 Flame emission spectroscopy

In order to obtain a more detailed insight into the chemistry of the hypergolic combustion, flame emission spectroscopy was carried out during ignition and rapid combustion of the propellants. By stitching together and summing up multiple spectral measurements, several spectra for the hypergolic flame emission of HTP and EMIM SCN with varying degrees of Cu SCN added were obtained. The 600 g/mm grating was used for optimal results. Each of these spectra consists of data from at least 50 ignition events. FIG. 7 shows a spectrum of an ignition event of pure EMIM SCN and a spectrum of an ignition with 5 wt.% Cu SCN added to the fuel.

Alkali metals

Both depictions in FIG. 7 are dominated by two emission bands, the sodium (588.9 nm and 589.5 nm) and potassium (766.4 nm and 769.8 nm) doublets. The former is a synthesis remnant that

causes the orange flame colour. This bright emission band consists of the well-known Na D_1 and D_2 lines. The degeneration of both the Na and K band is caused by the two possible rotational states of the outer shell electron (parallel and anti-parallel to the nucleus rotational axis). Its Boltzmann distribution can be applied for temperature determination. However, time and spatial resolution of the measurements were not sufficient for a conclusion regarding thermal equilibrium which is prerequisite for thermal measurements.

However, emission spectra recorded during the ignition process of EMIM SCN with the added catalyst show a variety of copper and copper oxide lines (FIG. 8). Furthermore, traces of Lithium (doublet at around 670.7 nm) were also revealed by flame emission spectroscopy.

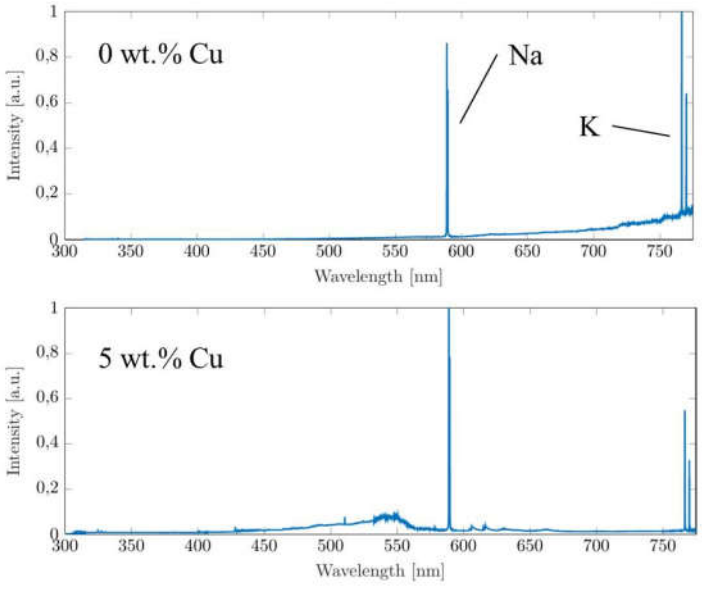

FIG. 7: Flame emission spectra for the hypergolic ignition without catalyst (above), and with 5 wt.% Cu catalyst (below). Sodium and potassium lines clearly dominate the visible wavelength regime.

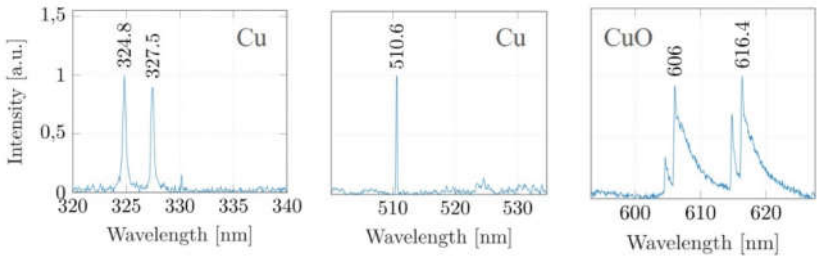

FIG. 8: Spectral details recorded during ignition with 5 wt.% Cu additive.

The OH* band

The ultraviolet regime of the spectrum was dominated by the emission band of the OH radical: A short-lived combustion product that emits depending on the pressure in a nonlinear manner (Fiala et al. 2020). The spectrum depicted in FIG. 9 was recorded using a grating with 1,800 gr./mm. The amount of Cu in the liquid fuel EMIM SCN was 5 wt.%. It reveals three major emission lines. G_{ref} is a temperature invariant signal yet G_0 and G_1 change their intensities for different flame temperature values (Pellerin et al. 1996; Stützer et al. 2019).

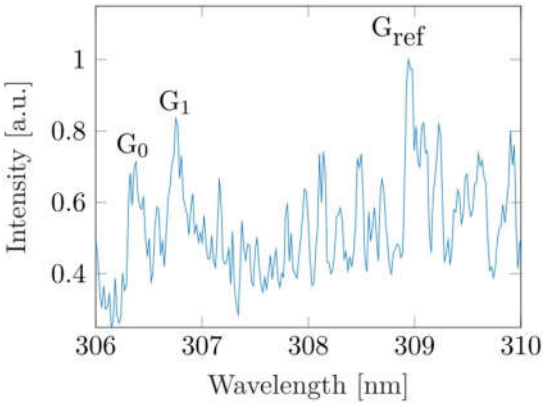

FIG. 9: UV-regime of the flame emission spectrum. The line G_{ref} is temperature invariant while G_1 and G_0 differ in their intensity regarding flame temperature (Pellerin et al. 1996; Stützer et al. 2019).

TABLE 3: Measured intensity ratios of the variable emission lines G_0 and G_1 regarding G_{ref} as well as the derived flame temperature for all three values of the added amount of Cu SCN.

	0 wt.% Cu SCN	**1 wt.%** Cu SCN	**5 wt.%** Cu SCN
Int. G_0/G_1	0.77	0.79	0.86
T [K]	2,800	2,900	3,300

This characteristic behavior was applied to determine flame temperature for the combustion of EMIM SCN with a fraction of 0 wt.%, 1 wt.% and 5 wt.% Cu. Results are shown in TABLE 3.

It was found that an increased fraction of the Cu catalyst results in an increased flame temperature. However, due to a relative uncertainty in the spectral resolution the systematic error of the temperature values was estimated 10%. Each spectrum was corrected using a previously derived devise function. Furthermore, the recorded data were background and flat field corrected. All temperature values were in accordance with models generated using LIFBASE software for temperature and pressure dependent emission of diatomic molecules (Luque and Crosley 1999).

4. CONCLUSION

The previously described experiments proved the ability for hypergolic ignition of highly concentrated hydrogen peroxide with EMIM SCN. This is a decisive step towards the replacement of the toxic and dangerous hydrazine derivates with environmentally friendly and less toxic propellants. Moreover, the copper additive dissolved in the ionic liquid accelerated the reaction and increased the flame temperature.

The new drop test chamber proved its ability for versatile experiments on hypergolic ignition tests. However, future investigations will be conducted using an extended parameter range. Pressure and temperature inside the chamber are to be systematically varied and examined. Particular attention has to be paid for further improvement of combustion and ignition performance. New catalysts have to be tested and the time resolution of the optical methods will be increased in order to better understand the reaction chemistry.

REFERENCES

De Izarra, C., (2000) UV OH spectrum used as a molecular pyrometer, *J. Phys. D: Appl. Phys.,* **33**(14), pp. 1697–1704.

Pellerin, S., Cormier, J.M., Richard, F., Musiol, K., and Chapelle, J., (1996) A Spectroscopic Method Using UV OH Band Spectrum, *J. Phys. D: Appl. Phys.,* **29**(3), pp. 726–739.

Nonnenberg, C., Frank, I., and Klapötke, T.M., (2004) Ultrafast Cold Reactions in the Bipropellant MMH/NTO: CPMD Simulations, *Angew. Chem. Int. Ed.,* **43**, pp. 4585–4589.

Catoire, L., Chaumeix, N., and Paillard, C., (2004) Chemical Kinetic Model for MMH/NTO Gas-Phase Combustion and Hypergolic Ignition, *J. Propuls. Power,* **20**(1), pp. 87–92.

Catoire, L., Chaumeix, N., Pichon, S., and Paillard, C., (2006) Visualizations of Gas-Phase NTO/MMH Reactivity, *J. Propuls. Power,* **22**(1), pp. 120–126.

Stützer, R., Kraus, S., and Oschwald, M., (2020) Investigation of Optical Laser Beam Impairment on Hypergolic LunarLander Exhaust Plumes for a Lidar Feasibility Study, *CEAS Space Journal,* **12**, pp. 481–487.

Stützer, R., Bublies, S., Mayer, T., Kraus, S., Clauss, W., and Oschwald, M., (2013) Optical Investigation on the Hypergolic MMH/NTO Combustion in Spacecraft Propulsion, in *5th European Conference for Aeronautics and Space Sciences (EUCASS).* Munich, Germany.

Matsumoto, M., Kano, H., Suzuki, M., Katagiri, T., Umeda, Y., and Fukushima, S., (2016) Carcinogenicity and Cronic Toxicity of Hydrazine Monohydrate in Rats and Mice by Two-Year Drinking Water Treatment, *Regul. Toxicol. Pharmacol.,* **76**, pp. 63–73.

Mellor, B., (2004) in *2nd Int. Conf. on Green Propell. for Space Prop.* (ESA SP-557). Sardinia, Italy.

Lauck, F., Negri, M., Freudenmann, D., and Schlechtriem, S., (2020) Selection of IL and Characterization of Hypergolicy with Hydrogen Peroxide, *Int. J. of Energetic Materials and Chem. Propuls.,* **19**, pp. 25–37.

Lauck, F., Negri, M., Freudenmann, D., and Schlechtriem, S., (2019) Study on Hypergolic Ignition of Ionic Liquid Solutions, in *8th European Conference for Aeronautics and Space Sciences (EUCASS).* Madrid, Spain.

Lauck, F., Balkenhohl, J., Negri, M., Freudenmann, D., and Schlechtriem, S., (2021 (a)) Ignition Investigations of a Novel Hypergolic Ionic Liquid with Hydrogen Peroxide Drop Tests, in *7th*

Space Propulsion Conference.

Balkenhohl, J., (2019) Design, Construction and Commissioning of a Reaction Chamber for Hypergolic Fuels as well as First Optical Measurements of the Flame Emission, Master's Thesis. Institute of Space Systems, University of Stuttgart, Germany.

Lauck, F., Balkenhohl, J., Negri, M., Freudenmann, D., and Schlechtriem, S., (2021 (b)) Green bipropellant development – A study on the hypergolicity of imidazole thiocyanate ionic liquids with hydrogen peroxide in an automated drop test setup, *Combustion and Flame,* **226**, pp. 87–97.

CCD30-11 Front Illuminated Open Electrode High-Performance CCD Sensor Datasheet. (2013). A1A-100008 Version 10. e2v Technologies Ltd.

Fiala, T., Sattelmayer, T., Gröning, S., Hardi, J., Stützer, R., Webster, S., and Oschwald, M., (2020) Comparison Between Excited Hydroxyl Radical and Blue Radiation from Hydrogen Rocket Combustion, *J. Propuls. Power,* **33**(2), pp. 490–500.

Stützer, R., and Oschwald, M., (2019) The Hyperfine Structure of the OH* Emission Spectrum and its Benefits for Combustion Analysis, in *8th European Conference for Aeronautics and Space Sciences (EUCASS).* Madrid, Spain.

Luque, J., and Crosley, D.R. (1999) LIFBASE: Database and Spectral Simulation Program (Version 1.5). SRI International Report MP, 99.